

Supplementary Information for “Photon and Carrier Management Design for Nonplanar Thin-Film Copper Indium Gallium Selenide Photovoltaics”

Colton R. Bukowsky^a, Jonathan Grandidier^{a,b}, Katherine T. Fountaine^{a,c}, Dennis M. Callahan^{a,d}, Billy J. Stanbery^{e,f}, Harry A. Atwater^a

^aCalifornia Institute of Technology, 1200 E. California Drive, Pasadena, California 91125, USA

^bCurrently with the Jet Propulsion Laboratory, 4800 Oak Grove Dr., Pasadena, California 91109, USA

^cCurrently with Northrup Grumman Aerospace Systems, One Space Park Dr., Redondo Beach, California 90278, USA

^dCurrently with The Charles Stark Draper Laboratory, Inc., 555 Technology Square, Cambridge, MA 02139, USA

^eHelioVolt Corporation, 6301 E Stassney Ln, Austin, Texas 78744, USA

^fCurrently with Siva Power, 5102 Calle del Sol, Santa Clara, California 95054, USA

SI1: Anti-Reflection Coatings and Optimized Planar Device

Because it is commonly employed in experimental devices and in order to find an upper limit of device performance for the electrical parameters used, the optimum MgF_2 Anti-Reflection Coating (ARC) thickness was found by optimizing for photocurrent absorbed in the CIGS material. For planar and structured devices, the optimum thickness was 110 nm, while for the periodic device, the optimum was 166 nm. Figure S1a compares the 700 nm device with ARC (cp. Structured device with $t=0$ nm), the 1.7 μm device with ARC (cp. Structured device with $t=1000$ nm), and a planar 2.9 μm device with ARC. The 2.9 μm planar device with ARC was the optimal CIGS thickness found by parameterizing the CIGS thickness with the figure of merit being efficiency in order to compare to the devices studied. Figure S1b shows that when adding the dielectric spacer layer to devices with optimized ARC, the thin planar device out-performs the optimized planar device in the case of perfect CIGS| SiO_2 interface passivation. The decreased reflection in the planar 700 nm device increases the current, and therefore efficiency, compared to Figure 4. The same is true of the other devices. The randomly textured device performs best of the three. These curves show the added benefit of dielectric layers, but also recognize that if sufficiently low interface SRVs cannot be achieved, the optimum device will still be a thick planar device with ARC.

Figure S1c shows the CIGS absorption when the ARC is applied. Compared to Figure 3c, the optimum ARC for planar and structured devices maximizes absorption near the peak of the photocurrent flux in the solar spectrum between 600-800 nm, with the optimum ARC coating being 110 nm thick. The periodic

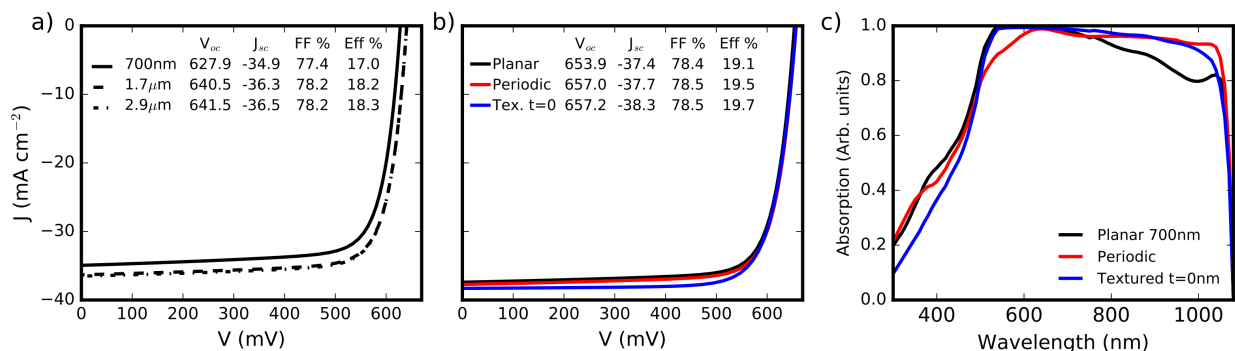


Figure S1: **Devices with Anti-Reflection Coatings** a) The JV curves of planar device with 110 nm MgF_2 ARC. The thicker optimized 2.9 μm device shows a minor improvement over the 1.7 μm textured device, corresponding to the planar equivalent thickness of a textured device with $t=1000$ nm b) The planar, periodic, and textured devices with a 190 nm dielectric layer at the back-contact and ARC outperform even the optimized planar device. Inset of a) and b) show the J-V parameters of the devices. c) the CIGS absorption spectra for the ARC coated devices in b).

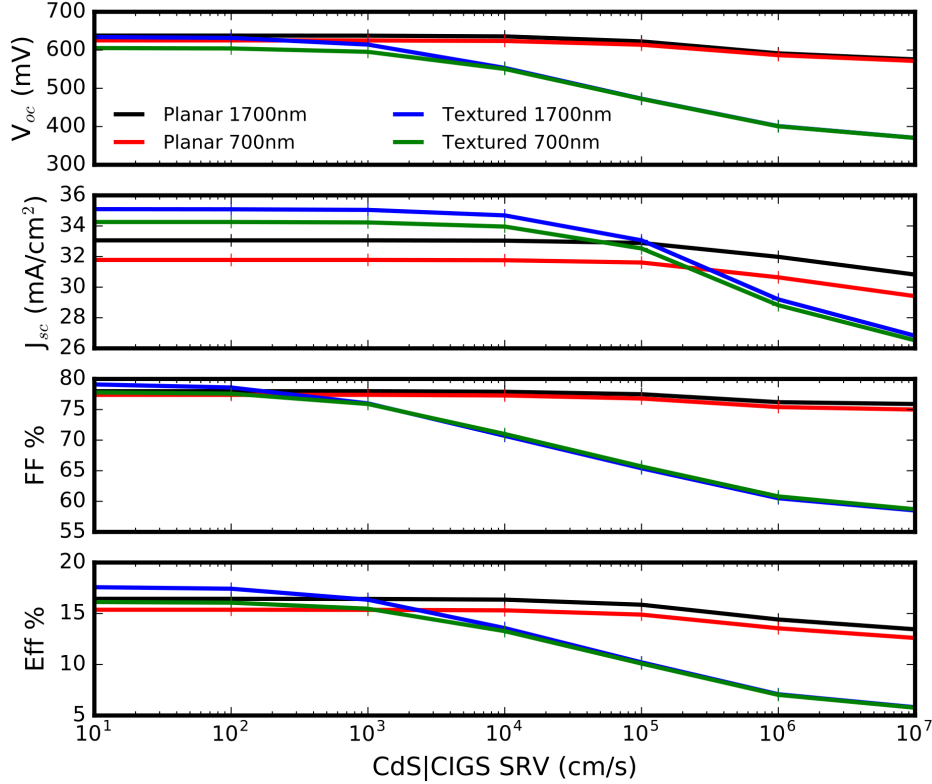


Figure S2: **Recombination at Junction for Planar and Textured Devices** Variation of the surface recombination velocity at the CIGS|CdS interface for different architectures and thicknesses reveal that the textured CIGS absorber outperforms a traditional planar geometry for moderate SRV values, but steeply declines in performance as the SRV begins to become the dominant recombination mechanism due to increased junction interfacial area.

device has an optimum ARC thickness of 166 nm. The periodic texture already enhances the absorption response between 600-800 nm significantly, leading to an ARC tuned to about 900 nm having the most additional effect. The large attenuation coefficient of CIGS leads to decoupling of the multiple photon management strategies in this device, and enables the periodic pattern, the ARC, and the dielectric layer to be separately active in different parts of the spectrum. The absorption peak due to the periodic pattern centered around 700 nm is not significantly affected by the ARC (nor is the near band-edge enhancement of the dielectric layer) as one would expect if the two were resonantly coupled. A better optimization would co-optimize the periodic pattern, the ARC, and the dielectric layer simultaneously, since it is unclear whether or not the ARC or periodic texture is the more effective strategy between 600-800 nm. However, the absorption response in S1c demonstrates how the enhancement effects can be superimposed as long as they are sufficiently decoupled.

SI2: Effect of Increased Junction Interfacial Area

There is justified concern that the increased junction interface would increase the junction recombination. A sensitivity analysis was performed for this parameter for the textured and planar CIGS devices. The increased junction does show the textured devices being more sensitive to the textured junction for increasing surface recombination velocity (SRV), as shown in Figure S2. For SRVs at the CIGS|CdS interface up to $\sim 10^3$ cm s⁻¹, the textured geometry outperforms the planar geometry due to its ability to collect significantly more photocurrent. The thinner and thicker devices show the same trends in both devices, and the

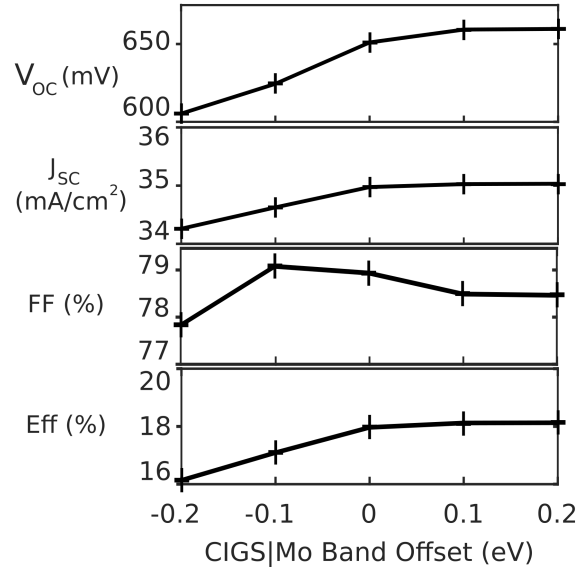


Figure S3: **Sensitivity to Absorber|Back-contact Band Offset** Randomly textured device (planar equivalent of 700nm, Figure 1b) sensitivity to the back-contact band offset. Minimizing the negative bending of the conduction band in CIGS allows more photogenerated minority carriers to reach the junction (J_{SC}) and enables a larger concentration of excited carriers to be maintained (V_{OC}).

efficiency becomes independent of thickness as surface recombination becomes the dominant recombination mechanism for the textured devices. The fill factor and voltage are most affected by increases in junction recombination, with fill factor being the first parameter to show decline as charge carriers find recombination sites before being able to cross the junction. The periodic structure was not parametrically studied here, but its interfacial area is between that of the textured device and the lower limit of the planar device; the performance of such a device would be bounded by the results given here.

SI3: CIGS|Mo Band Offset

The back-contact passivation by dielectric separation layers in sub-micron thickness CIGS films is only required when a band offset exists between the CIGS and the Mo contact, which was -0.2 eV for all electronic results presented thus far.[1] A thin layer of MoSe_2 is sometimes used to create an indirect Ohmic contact to Mo.[2] Gallium grading has also been proposed to avoid minority carrier loss to the back contact.[3] We examined the sensitivity of the randomly textured CIGS device with 700 nm planar equivalent thickness to this offset in Figure S3. A -0.2 eV offset corresponds to a ~ 50 mV loss in V_{OC} compared to a V_{OC} of 651 mV for zero band offset. A $V_{OC}=660$ mV is observed for more positive offsets, and a maximum efficiency of 18.1% is achievable in randomly textured CIGS devices studied. For a band offset of 0 V, the contact is mildly selective to majority carriers, and this effect further increases with positive offset. As the selectivity of the contact increases, the concentration of excited carriers does so, leading to larger quasi-fermi level splitting. The J_{SC} follows the open circuit voltage, as more carriers are can be collected at the junction. The fill factor remains relatively constant with varying band offset. Thus, creating Ohmic or selective contact is another viable route to reduction of minority carrier recombination in sub-micron CIGS absorbers, and again highlights the importance of the back-contact properties for very thin CIGS.

References

- [1] M. Gloeckler, A. L. Fahrenbruch, J. R. Sites, Numerical modeling of CIGS and CdTe solar cells: setting the baseline, in: Proceedings of 3rd World Conference on Photovoltaic Energy Conversion, 2003.
- [2] B. J. Stanbery, Copper Indium Selenides and Related Materials for Photovoltaic Devices, *Critical Reviews in Solid State and Materials Sciences* 27 (2) (2002) 73–117. doi:10.1080/20014091104215.
URL <http://www.tandfonline.com/doi/abs/10.1080/20014091104215>
- [3] B. Vermang, J. T. Wätjen, V. Fjällström, F. Rostvall, M. Edoff, R. Gunnarsson, I. Pilch, U. Helmerson, R. Kotipalli, F. Henry, D. Flandre, Highly reflective rear surface passivation design for ultra-thin Cu(In,Ga)Se₂ solar cells, *Thin Solid Films* 582 (2015) 300–303. doi:10.1016/j.tsf.2014.10.050.
URL <http://linkinghub.elsevier.com/retrieve/pii/S0040609014010116>